MOEM

Modern Electronic Materials 2020; 6(3): 113–123
DOI 10.3897/j.moem.6.3.54583

Research Article

Europium monoxide as a basis for creating a high-temperature spin injector in the semiconductor spintronics

Arnold S. Borukhovich[1]

1 Russian State Vocation Pedagogical University 620012, Yekaterinburg, Russia

Corresponding author: Arnold S. Borukhovich (super.arnold15@yandex.ru)

Received 22 May 2020 ♦ **Accepted** 6 June 2020 ♦ **Published** 30 September 2020

Citation: Borukhovich AS (2020) Europium monoxide as a basis for creating a high-temperature spin injector in the semiconductor spintronics. Modern Electronic Materials 6(3): 113–123. https://doi.org/10.3897/j.moem.6.3.54583

Abstract

The results of the creation of a high-temperature spin injector based on EuO: Fe composite material are discussed. Their magnetic, electrical, structural and resonance parameters are given in a wide range of temperatures and an external magnetic field. A model calculation of the electronic spectrum of the solid solution Eu–Fe–O, responsible for the manifestation of the outstanding properties of the composite, is performed. The possibility of creating semiconductor spin electronics devices capable of operating at room temperature is shown.

Keywords

composite, europium monoxide, magnetic semiconductor, magnetization, spintronics, spin-polarized current transport, super paramagnetizm.

1. Introduction

In the practice of creating real spintronic structures and spin transistors of cryogenics, as is known, so-called dilute magnetic semiconductors **(DMS)** are widely used. These are semiconductor alloys containing magnetically active ions of manganese: $Be_xMn_yZn_{1-x-y}Se$ (x = 0.07, y = 0.03, $T_c \approx 7$ K), $Ga_{1-x}Mn_xAs$ (x = 0.045, $T_c \approx 52 \div 110$ K), $Cd_{1-x}Mn_xGeP_2$ (T_c = 320 K) and some others [1–3]. These alloys themselves have a low saturation magnetization and the same degree of spin polarization of intrinsic charge carriers (only a few scores of percent). The introduction into the structure of basic wide-gap non-magnetic semiconductors of magnetic manganese ions creates the prerequisites for Zeeman splitting of the electronic energy levels in them. The magnitude of such a Zeeman splitting at the similar crystals is determined by the relation [4]:

$$\Delta E = A_{sd} x S_0 B_s \left[\mu_B s g H \frac{(T - T_{eff})}{kT} \right], \quad (1)$$

where are: A_{sd} is an integral of *s-d* – exchange for conduction electrons; x is the concentration of the Mn magnetic ions; S_0 is their effective spin; B_s is the Brillouin function; μ_B is Bor's magnetron; T_{eff} is the effective spin temperature of magnetic ions; s is the spin of the charge carriers. Some compositions of such DMS have record-high values of the g-factor of conduction electrons for semiconductors. For example, in the first of the aforementioned $g \approx 100$. All of this serves to realize the spin current-carrying over the Zeeman levels of such crystals without a spin-flip. Moreover, the uniformity and similarity of the crystal lattices parameters of similar DMS with basic nonmagnetic semiconductor phases allows constructing the superlattices from them using planar technology, for example, by molecular beam

epitaxy, and layer-by-layer assembly. It was just such a construction of such structures that, as noted, it was possible to obtain Ga–Mn–Sb layered structures with $T_c \approx 400$ K, and also the structure of $Cd_{1-x}Mn_xGeP_2$ with a value of $T_c = 320$ K. It was supposed to create spintronic structures and spin transistors capable of operating at room temperatures, with their participation. However, this apparently did not succeed. The spintronic devices created on their basis could work steadily only at temperatures below 200 K [5]. In the first decade of this century, constructing of a suitable injector for spintronics covered the area of composite materials. In this case, the methods of film construction of similar materials were used, including methods of molecular beam epitaxy **(MBE)** and magnetron sputtering. As such composites, film structures made of alternating layers of titanium oxide (as well as zinc or silicon oxides) and metallic cobalt, retaining semiconducting conductivity at room temperatures are mainly used [6, 7]. Such structures are called "sandwich". They are characterized by the same significant values of the magnetoresistance effect which makes them promising in the development of devices with GMR or elements of quantum computers – another promising area of spintronics application. Created oxide "sandwich" structures are unusual in that they are based on non-traditional materials for the needs of electronics – oxides of transition elements, previously not found proper use in physical materials science. If the properties of such structures turn out to be reproducible and stable, then the methods of designing spintronic materials have broad prospects. Indeed, among titanium oxides, only tetragonal phases of anatase and rutile are semiconductors with a band gap of 3.2 and 3.0 eV, respectively, and titanium monoxide, TiO, has metallic electric conductivity and, as a consequence, is apparently less promising for specified goals.

The manifestation of ferromagnetism with a Curie temperature exceeding room temperature in the anatase phase of $Ti_{1-x}Co_xO_2$ oxide has not been explained to this day. Although the mechanisms of its possible manifestation have been widely discussed in the literature [8–13], nevertheless the values of the magnetic and electric characteristics observed for this composite are insufficient for its use in spintronics.

2. Synthesis and properties of the EuO : Fe composite – high-temperature spintronics

Taking into account the results of the above works, the authors of the publications [14–17] synthesized bulk composite poly- and single-crystal materials including a matrix of "classical" ferromagnetic semiconductor **(FS)** with low values of T_c and micro- or nanoparticles of ferromagnetic metals with high T_c dispersed in it: Fe and Co. It was supposed to preserve to some extent the distinctive physical parameters of the EuO phase in the composite against the background of the high value of T_c, which is characteristic of these *d*-transition metals. As the practice has shown, composites of the (EuO) : Fe_y composition ($0.15 \le y \le 0.25$) are able to preserve the physical parameters inherent in their components in different temperature ranges, remaining magneto-heterogeneous semiconductor materials with a Curie temperature much higher than room temperature, both in bulk and thin-film states.

Here it is necessary to note the following. In the early 1970's when the problem of a possible increase in the Curie temperature of the EuO phase was actively solved, attempts were made to solve it by doping the monoxide with transition metals of the 7th group of the periodic system – Fe, Co, Ni [18]. This turned out to be impossible to synthesize bulk single-phase crystals: these metals practically did not dissolve in the monoxide lattice and did not form solid solutions with it. Only EuO films obtained by the MBE method and containing a small (up to 5% by weight) percent of the impurity of these ferromagnetic metals had Curie temperatures of $T_c = 150$–180 K, remaining quasi-degenerate semiconductors. Thus, in this case, the synthesis of a possible high-temperature spintronic (EuO) : Fe_y assumed the final product in the form of a composite – a multiphase and magneto-heterogeneous material – in advance.

Since it follows from the preceding that europium monoxide does not form a solid solutions with iron, the creation of the required composite at the dispersion of metallic iron particles in EuO was carried out by chemical reduction of a mixture of powders of sesquioxides of europium and iron during their high-temperature vacuum reduction in the presence of carbon, to the Europium monoxide state in the structure of NaCl, and metallic α-iron. Calculation of charges was carried out according to the reaction equation [17]:

$$Fe_2O_3 + Eu_2O_3 + 4C = 2Fe + 2EuO + 4CO\uparrow. \qquad (2)$$

The final products of the reduction of the mixture of higher oxides of iron and europium with carbon are fine magnetic powders consisting of 300 to 500 nm metal iron granules uniformly dispersed in the oxide matrix of EuO. Powders are stable in air during long-term storage, they are easily pressed into products of various shapes.

Annealing of the latter at 800 °C at pressure of 10^{-1} Pa for two hours does not cause a change in the chemical and phase composition of the material. Measurements of the nominal electrical resistivity of the composite were carried out at sintered samples of rectangular shape at room temperatures. According to these data (Fig. 1), the area of the composite compositions corresponding to the semiconductor character of their conductivity was determined and comprised from 15 to ~25% of Fe mass in a mixture with EuO. It was at the samples from this region of composite compositions that all measurements of physical quantities were performed, as presented below, as meeting the necessary requirements for semiconductor spintronic materials.

Thus, the value of the activation energy of the composite (ΔE) was estimated from the position of the absorption edge on the optical transparency curve – it corresponds to

a value of $\Delta E \approx 0.75$ eV [17] that is characteristic for the doping of this monoxide. In the "pure" EuO $\Delta E = 1.2$ eV [19]. Figure 2 shows the field dependence of the ferromagnetic saturation moment of a composite of the $(EuO)_{0.75}Fe_{0.25}$ composition at $T = 2$ K and $T = 300$ K, and its temperature dependences are shown in Fig. 3.

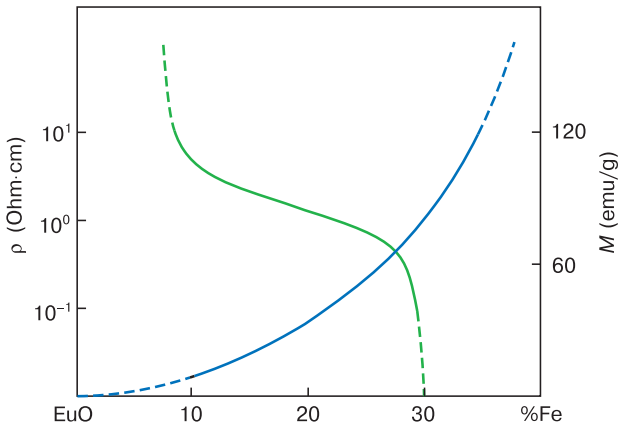

Figure 1. Dependences of the nominal of the specific electric resistivity (ρ) and the ferromagnetic saturation moment (M) of the EuO : Fe composite on composition.

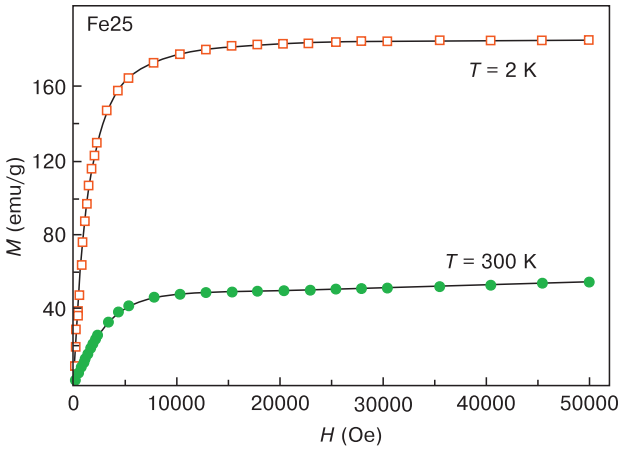

Figure 2. Dependence of the magnetic saturation moment for $EuO_{0.75}Fe_{0.25}$ composite.

From these data, it follows that the composite really is a heterogeneous mixture of two ferromagnets. Moreover, the value of the magnetization of the Fe component for this concentration range almost linearly corresponds to its share presence in the composite. At the room temperature, the ferromagnetic saturation moment of this composition composite is close to the value of $M \approx 60$ emu/g, which completely corresponds to the Fe-component, although it exceeds it in absolute terms by approximately 10÷15 units. At low temperatures the ferromagnetic moment predominates mainly due to the contribution of the divalent europium ion in the composite against which the contribution of iron to M is ≤ 30%. Throughout the temperature range the samples of the composite exhibit the properties of magnetically soft ferromagnet. A feature of the $M(T)$

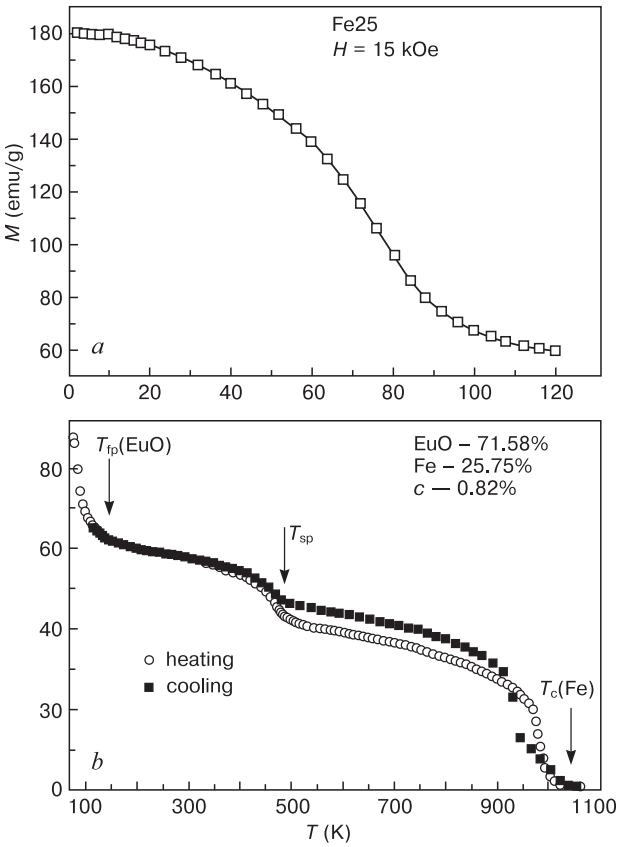

Figure 3. Temperature dependences of the magnetization of a composite at low (a) and elevated temperatures (b).

dependence in Figure 3 (b) is its inflection in the region of $T \approx 480$ K which is characteristic of the ferromagnetic disordering of the magneto-structural phase. If a transition of the ferro-para phase of the EuO takes place in the region of $T \approx 70$ K, and a similar for the Fe-component of the composite at $T \approx 1000$ K, then a certain ferromagnetic (superparamagnetic) constituent (i.e., ferromagnetic phase) of the composite must undergo a disorder in the above temperature range. Namely, it must be responsible for the increased value of its specific magnetization in the region of room and above (up to 480 K) temperatures. As will be shown below, such a component can be the ability of iron atoms under the conditions of synthesis of the EuO : Fe composite [20] to partially interact chemically with europium atoms via the indirect d–f-exchange interaction mechanism [21] with the formation of ferromagnetic Eu–Fe–O clusters (the $Eu_{1-x}Fe_xO$ solid solution, **SS**).

The synthesized volumetric samples of the $(EuO)_{1-x}Fe_x$ composites were further used as precursors for obtaining thin crystalline nanoscale films applied to different substrates: InSb (001), GaAs (100), and Si (111) single crystals, and also optical glass. Before the deposition the substrates were pretreated with a plasma of a microwave discharge in a successively changing working medium of oxygen, hydrogen, and argon at a pressure of ~ 0.1 Torr. The process of sputtering itself was performed on the developed methodologies with using standard vacuum deposition techniques [22]. The following research results

mainly relate to films produced by a thermal spraying method ("flash technique" or "explosion"). The thickness of the films varied between 100 and 500 nm. Thickness measurements and analysis of the film surface by layer-by-layer sputtering of samples with a slow oxygen ion beam were carried out with the Femtoscan-001 atomic force microscope with a scanning field up to 5 × 5 μm^2 operating in a contact mode using CSC12 silicon cantilevers with a tip radius of less than 20 nm (MicroMasch Company). Almost all the reflections of the X-ray films are identified for the cubic EuO structure of the Fm3m space group (225) with the parameter of the elementary crystal cell of a ~ 0.516 nm close to the value of this parameter for europium monoxide. At the same time, weak intensity reflections – (110) and (200) – are observed, characteristic of the cubic structure of the spatial group *Imm* of pure Fe, indicating that in the EuO matrix only a partial dissolution of the iron oxide appears (Fig. 4).

Investigations of the surface morphology of the films showed that the samples on the InSb substrates are the most homogeneous, their root-mean-square roughness is less than 10 nm both in the initial state and with a decrease in thickness to 100 nm. With smaller film thicknesses, punctures were formed deep down to the *substrate material in the intergrowth regions of the islands composing the film, and differing in size as much as possible in the images of the atomic force microscope*. The films are characterized by the semiconductive character of the electrical conductivity with the activation energy, $\Delta E \approx 0.75$ eV. At room temperature, the specific resistivity of films with a thickness of 200÷500 nm had a value of $\rho \sim 2 \cdot 10^2 \div 4 \cdot 10^{-3}$ Ohm·cm [18].

The behavior of the magnetization of the composite films (Fig. 5) correlates well with the data in Figure 3 – the characteristic features of the $M(T)$ dependences also appear in the films. Their magnetization reversal curve under normal conditions in the easy direction is close to rectangular, saturation is achieved in fields of $H \approx 0.5$ T (Fig. 6). However, the opening of the hysteresis loop is not observed. The magnitude of the magnetic moment of the composite thus reaches $M \approx 4\mu_B$ and correlates in these conditions with magnetically active Fe-centers in it. This value of M exceeds the characteristic value of the magnetic moment of pure iron almost by 20%, which completely corresponds to the contribution made to it from the environment of the paramagnetic moments of europium ions. At the same time, studies of the $M(T)$ dependence upon cooling of the composite films at low temperatures in an external magnetic field (the FC condition) and without a field (the condition **ZFC**) revealed another feature – the presence in the latter case of an inflection of this dependence in the temperature region of $T = 25 \div 30$ K (Fig. 7). This so-called blocking temperature (T_{bl}) is the transition from the ordered state to superparamagnetism of α-iron nanoparticles in the composite. Physically this means that the magnetic moments of such particles with $T \leq T_{bl}$ are antiferromagnetic in relation to ferromagnetically ordered state of the ions of the Eu^{2+} matrix. This leads to a general decrease in the magnetic moment of the composite at $T = 0$ K.

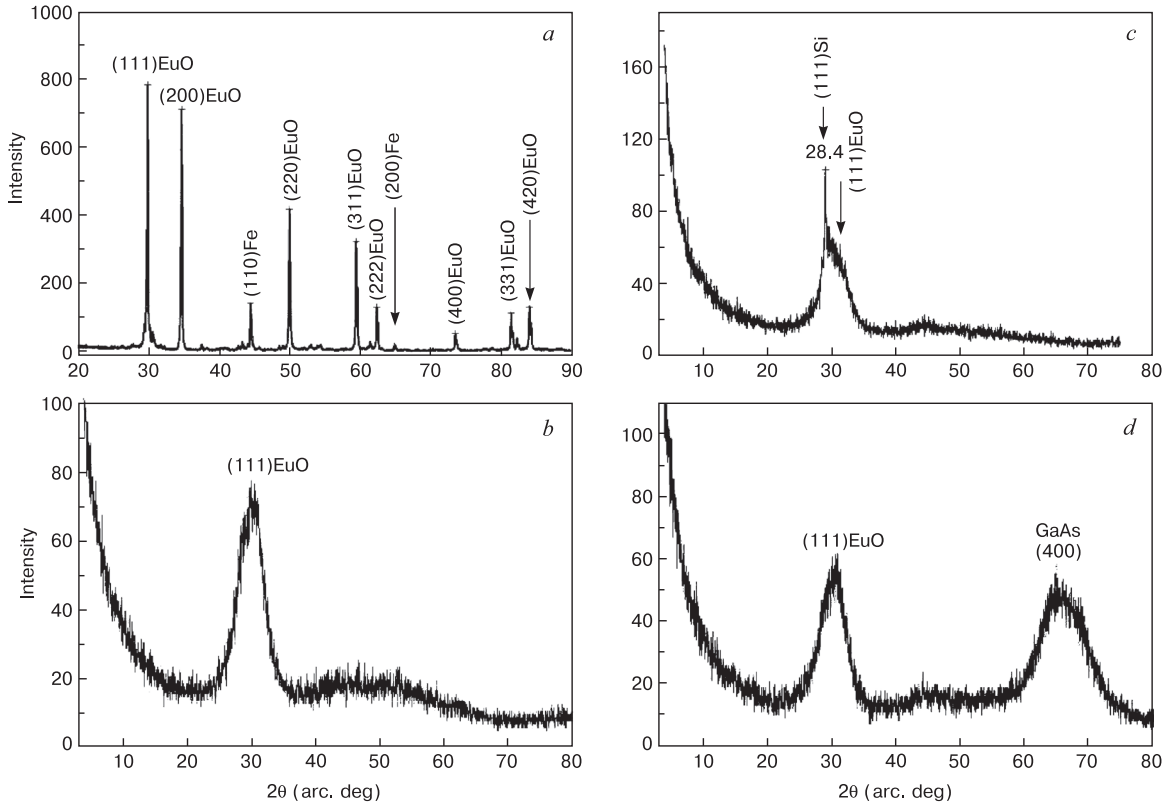

Figure 4. *X*-ray patterns of synthesized film samples: (*a*) the starting powder of the target EuO (25%) Fe; (*b*) EuO/Fe film on InSb (001); (*c*) EuO /Fe film on silicon (111); (*d*) is a film of EuO/Fe on GaAs (111). Indication of reflexes by data [23].

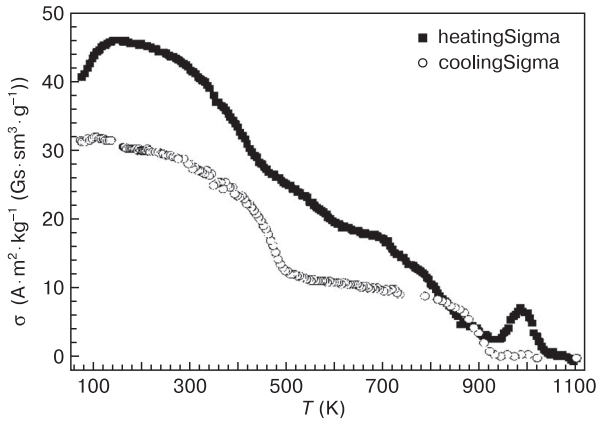

Figure 5. Temperature dependence of the composite films magnetization (d = 480 nm) on the InSb substrate.

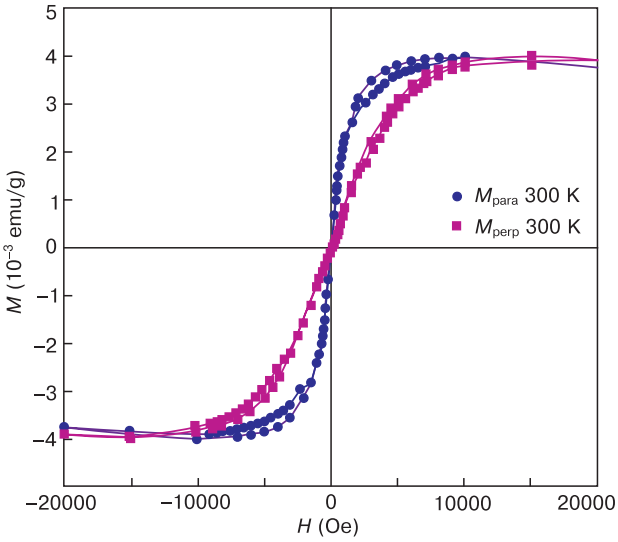

Figure 6. Magnetization curves of the composite film in contact with GaAs: along the contact plane (easy direction, para) and perpendicular (difficult direction, perp) at room temperature.

3. Studies of the EuO : Fe spintronic material using Mossbauer spectroscopy

To detail the results of magnetic studies of EuO : Fe composites, a study of their nuclear gyromagnetic resonance (**NGR** or Mossbauer) spectra on the ^{57}Fe and ^{151}Eu isotopes was made [24, 25]. The Mossbauer spectra were recorded on MS-2201 spectrometers at room temperature with ^{57}Fe and $^{151}Sm_2O_3$ sources. In this case, the iron spectra were recorded both on the polycrystalline powder of the composite and on films of the same composition up to 500 nm thick. The Eu-151 spectra were obtained only on powders.

Figure 8 shows the Mossbauer spectra of the ^{57}Fe bulk samples of the composite, made in the form of a powder (*P*). They contain at least two sixes of Zeeman lines: one with H_{eff} = 32.8 T, δ = 0, ΔE = 0, the other one with H_{eff} = 19.2 T, δ = +0.20 mm/s, ΔE = 0.005 mm/s, corresponding respectively to α-Fe and Eu–Fe–O clusters. The relative intensity of the sextets I(α-Fe) ≈ 0.72; I(Eu–Fe–O) ≈ 0.28. From which it can be concluded that the presence of iron in the composite, basically, corresponds to its free (metallic) state. The fraction of ferromagnetic clusters in it is much smaller, which agrees with the impossibility of formation of solid substitution solutions of Eu on Fe at the EuO lattice. The manifestation of the ionic state of iron in the composite should be considered as impurity centers forming Eu–Fe–O clusters as a result of a possible chemical bond in accordance with the mechanism noted in Section 2.

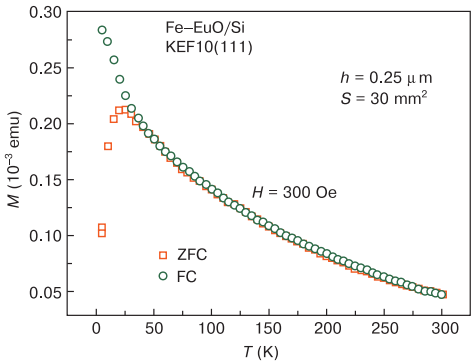

Figure 7. The magnetization of the $(EuO)_{0.75}Fe_{0.25}$ composite film on a silicon substrate under conditions of ZFC and FC.

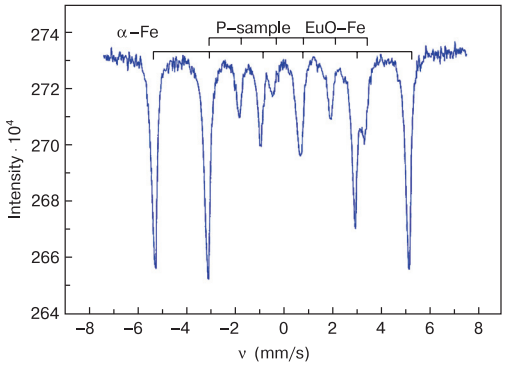

Figure 8. NGR spectra of ^{57}Fe powder of the EuO : Fe composite at room temperature.

The Mossbauer spectra of ^{57}Fe of the composite films (Fig. 9) represent a singlet with an isomeric shift of δ = +0.20 mm/s and a very weak splitting, typical for the manifestation of superparamagnetism of α-Fe nanoparticles.

The Mossbauer spectrum of the ^{151}Eu powder of the composite is illustrated in Fig. 10. It is an overlap of two lines characterized by isomeric shifts of δ = –12.6 mm/s and δ = + 0.02 mm/s, and width at half-height of 3.7 mm/s and 4.1 mm/s, respectively. The first line corresponds to the paramagnetic ion of the Eu^{2+} matrix, the second line is responsible for the manifestation of the valence state of Eu^{3+}. Such isomeric shifts of NGR spectra of ^{151}Eu in the composite correspond to the positions of these cations in the lattices of EuO and Eu_2O_3 [26]. The obtained spectra and the position of the isomeric shifts of the Eu^{2+} and Eu^{3+} ions in them agree well with the NGR investigation of the microcrystals of the magnetic semiconductor EuS interspersed in thin films of the TiO_2, Al_2O_3 and SiO_2 oxides [27].

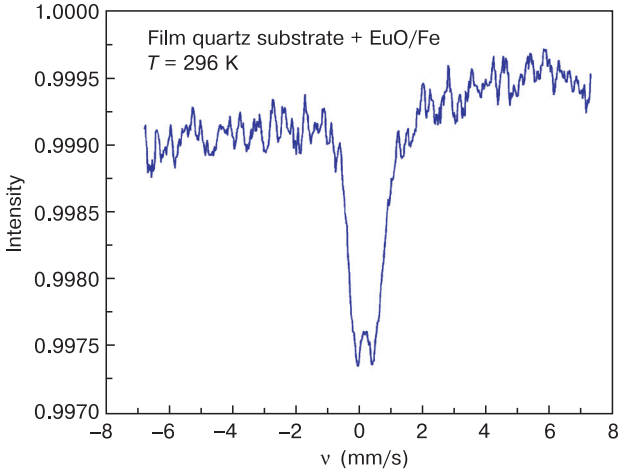

Figure 9. Mossbauer spectra of ^{57}Fe thin films of a composite on Quartz.

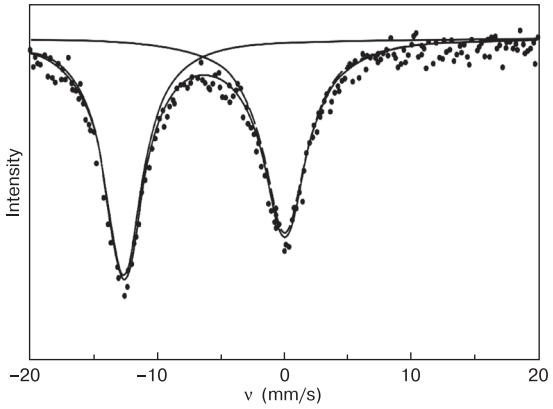

Figure 10. The Mossbauer spectrum of ^{151}Eu powder of the composite at room temperature.

The presence of Eu^{3+} ions in the composite, on the one hand, can be considered as an impurity phase of Eu_2O_3 due to the conditions of its synthesis – high-temperature reduction of a sesquioxide or a mixture (Eu_2O_3 + Fe_2O_3) by carbon. Based on the results of chemical and *X*-ray spectral analysis, the presence of this phase in the composite did not exceed 1% by weight.

On the other hand, comparison of state line intensities of the Eu^{3+} ions (~0.55) in the spectrum with that for the ion state Eu^{2+} (~0.45) may indicate the appearance in the composite of some "inductive" effect associated with the effect of iron atoms on the electron density on ^{151}Eu nuclei. This, as noted above, can correspond to the manifestation of an indirect (via the *p*-state of oxygen) *d–f* exchange between iron and europium to form Eu–Fe–O clusters. A possible, even partial, transfer of the electron density from Eu^{2+} to the iron will lead to the polarization of the spins of these ions, which under these conditions is equivalent to the manifestation of their ionic state in the cluster as Eu^{3+}, and the states of the iron ion as Fe^{+}. As a result, the ferromagnetic moment of such an $Eu^{3+}Fe^{+}O$ cluster at $T > 70$ K (the temperature of the ferromagnetic disordering of the EuO phase) due to the spin polarization of the paramagnetic europium ions from the nearest environment of the impurity Fe^{+} ion and localized on it is increased. As follows from the above mentioned magnetic data, numerically it exceeds the ferromagnetic moment inherent in pure iron at these temperatures by more than 10 units (in the SI system). And this, as noted, leads not only to an increase in the specific magnetization of the composite at room temperature, but and makes it a record among all other known materials, especially semiconductor, recommended for spintronics. When using a composite as a spin injector, these properties will be to contribute an increasing in the share of spin current transfer at spintronic structures created with its participation.

4. Electronic band structure of the $Eu_{1-x}Fe_xO$ solid solution. Calculation and comparison with the experimental data for the EuO : Fe composite

For a possible theoretical justification and understanding of the behavior of the experimental parameters of the EuO : Fe composite, the electronic band structure of the $Eu_{1-x}Fe_xO$ solid solution **(SS)** structurally included in its composition was calculated in comparison with the same calculation for "pure" europium monoxide [28]. As before, the calculation method included the use of the linear method of associated plane waves (FLAPW, code WIEN2k) with the generalized gradient approximation **(GGA)** of the exchange-correlation potential [29]. In recent years, a similar calculation method has been applied to the EuO and EuS phases doped with REM metals and provides fairly good correlation with experiment [30, 31].

In calculating [28] the concentration of iron doping of europium monoxide was 6.25% and 12.5%. In the original crystal, a NaCl cubic type cell of EuO consists of the same-named cations of the *f*-metal (Eu^{2+}). In the calculations a superlattice was constructed, obtained by translating the unit cell of EuO along the crystallographic axes when one of the europium cations is replaced by an iron ion. We recall that the essence of this method consists in the separation of the unit cell space into atomic **MT** (muffin-tin) spheres and interstitial regions, and the representation of wave functions in the form of a linear combination of spherical harmonics inside MT spheres and plane waves in the interstitial space. A mixed set of plane waves was used in the calculations.

The radii of the atomic spheres were 0.21 nm, the total number of **k** points in the irreducible part of the Brillouin zone for a composition with a concentration of 12.5% Fe was 72, and for a composition with a 6.25% Fe – concentration of 32. The resultant magnetic moments on Fe ions were 3.74μ_B, on Eu^{2+} cations – 6.88÷6.885μ_B, and on Eu^{3+} – 6.86÷6.875 μ_B. This is all under conditions of T = 0 K. The final results of the calculation of the SS electronic band structure at the spintronics composite are shown

in Figs 11–13. But before proceeding to the analysis of the performed calculations it is necessary to note the following. It is known that in case of systems with strongly correlated electrons which are also europium compounds, the GGA-approximation makes calculations for large elementary cells possible, but it requires certain corrections for correct description of the energy gap in the spectrum of band states. In this case, correlations of the band states spectrum in (GGA + U) – approximation are made [32]. This approach introduces corrections to the exchange-correlation potential for atoms that have valence electrons in sufficiently localized orbitals, which in our case are 4*f*- and 5*d*-orbitals of europium atoms and 3*d*-orbitals of iron atoms. The values of the corrections depend on the values of the U parameters of the Coulomb and J exchange interactions which are determined the most often by fitting the characteristics of the calculated band-state spectrum to the available experimental data. It is also known that the parameter J is much smaller than U and has little effect on the calculation results. Therefore, for all the mentioned orbitals, we assumed $J = 0$. For iron atoms, we used the value of $U = 5$ eV, proposed in [33] on the basis of calculations of the band structure of Fe_3O_4 by the FLAPW method. Exactly the same value of $U = 5$ eV was proposed for 4*f*- and 5*d*-orbitals of europium in [34] devoted to the calculation of the EuO band structure with allowance for correlation corrections. By varying these values within 1 eV near the value indicated above, we found that the optimal values for the europium orbitals are $U(4f) = 5.5$ eV and $U(5d) = 5$ eV, leading to a good agreement between the results of band calculations and the above experimental data.

The calculated densities of the band states for pure and iron-doped europium oxide shown in Figures 11 and 12 indicate that in both cases the band states formed mainly by the 2*p*-orbitals of oxygen atoms are located below the energy -2eV, whereas the band states formed by the 5*d*-orbitals of europium atoms (the energy of states is given relative to the Fermi level) are situated at the energy above 0.5 eV. The band states formed by the 4*f*-orbitals of europium are situated in the near Fermi region. In case of pure EuO the forbidden gap, i.e. the activation energy of the conductivity, between the Fermi level near the 4*f*-zone ceiling and the bottom of the 5*d* band is 0.8 eV, which agrees well with the experimental value of 1.2 eV [35]. Also the calculations reproduce well the interval between the maxima of the 2*p*O- and 4*f*Eu-states, equal to 2.5 eV [36].

The most significant changes in the spectrum of the EuO band states when doped with iron are the appearance of two bands of states with a positive spin-up direction at the energy near -6 eV and one band with a negative spin-down direction at Fermi level (Fig. 13). Differences between the band states obtained for the 32-atom supercell i.e., with replacement of europium with 6.25 at.% of iron, and band states for a 16-atom supercell, i.e., when replacing 12.5 at.% of iron, are insignificant, so we will consider the case of a 16-atom supercell. The magnetic moments obtained for this case on Fe ions were $3.74\mu_B$, and on Eu^{2+} cations they were from 6.86 to $6.88\mu_B$. To explain these

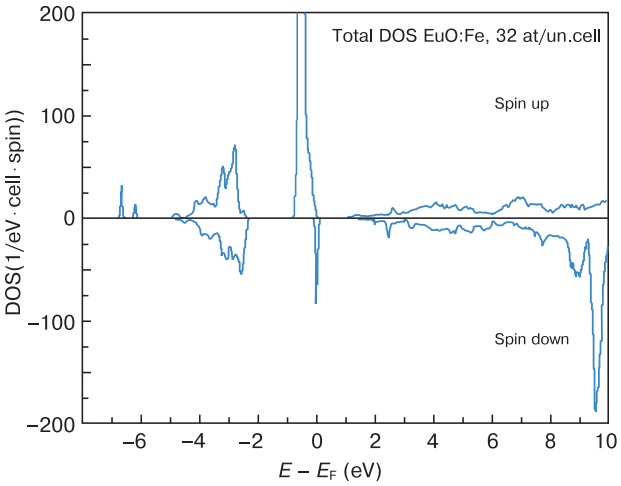

Figure 11. The density of electronic states of the $Eu_{1-x}Fe_xO$ solid solution with a dopant concentration of 6.5 at.%.

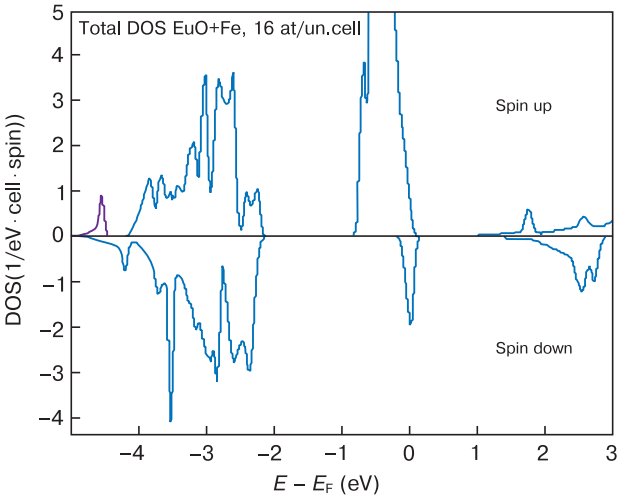

Figure 12. The density of electronic states of SS $Eu_{1-x}Fe_xO$ with a dopant concentration of 12.25 at.%.

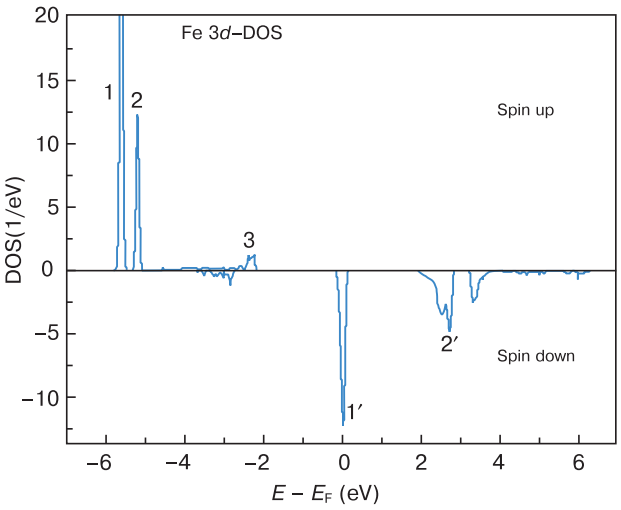

Figure 13. The density of the electronic *3d*-states of iron (according to Fig. 12 with the separation of the partial).

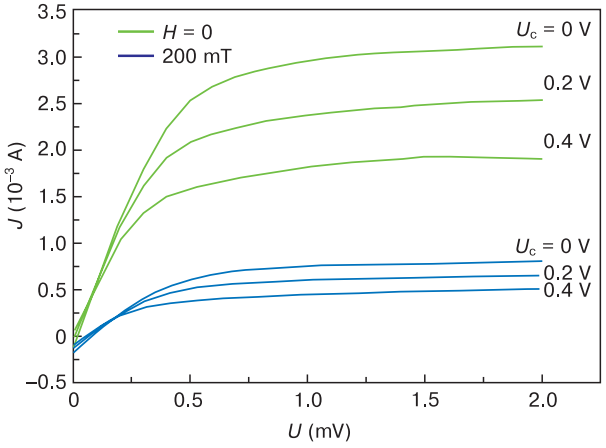

Figure 14. The current-voltage characteristics of a spin diode without a magnetic field and in a field of 200 mT (2 kOe)

values, we consider the partial density of the 3*d* states of iron atoms which additively enters the band spectrum of this SS (Fig. 14). The bands of spin-up band states noted on it by the numerals 1 and 2 have the type of local symmetry t_{2g} and e_g and contain 3 + 2 electrons. Another peak of the density of *3d*Fe-states (peak 3) is located at the top of the valence *2p*O-band, but it is a consequence of the hybridization of 2*p*O- and 3*d*Fe-states.

Band *1*' corresponds to spin-down *3d*Fe-states with e_g-type local symmetry: it contains one electron. Band *2*' corresponds to the empty zone of spin-down *3d*Fe states. It follows that the iron ions in the monoxide structure retain 6 electrons, i.e. they are in the charge state 2^+ and should have a magnetic moment equal to $4\mu_B$ which corresponds to the data given above. The spin-up band of the 4*f*-states in the near Fermi region contains ~ 7 electrons, i.e., the magnetic moment of the Eu atoms is ~ $7\mu_B$, which also corresponds to the values given above. Consequently, the formation of O^{2-} anions occurs due to electron transfer from the 4*s*-states of iron and 6*s*-states of europium. The reason for the presence of large magnetic moments on iron atoms is a large exchange splitting of the states of iron ions – at around 5 eV (Fig. 13), so that the majority of spin-down states of iron are not populated by electrons. As a result, the magnetic moment on Fe^{2+} cations is ~ $1.7\mu_B$ higher than the magnetic moment of pure iron. Accordingly, at room temperature, the numerical value of the saturation magnetization of the composite due to doping reaches values of 40÷60 emu/g (in the SI system) [15]. Since the 3*d*-orbitals of iron are much less localized in space than the 4*f*-states of europium, the appearance of iron atoms in the structure of the monoxide leads to an increase in the exchange interaction between the *f*- and *d*-cations and, as a consequence, to an increase in the Curie temperature of the composite. This makes Fe-doped europium monoxide the record one among all other known semiconductor ferromagnetic materials, recommended for spintronics as spins injectors, including at room temperatures. Note also that in the energy range from about 0.9 to 1.3 eV, i.e., near the bottom of the conduction band, there are no spin-down band states. This may mean that even in the presence of iron atoms a 100% spin polarization of the charge carriers is possible what corresponds to the previously indicated values of the spin polarization *P* in pure EuO [37].

It follows from the calculations that at low iron concentrations in EuO, its impurity electrons at states below the valence band, like spin-down electrons at the Fermi level, form rather narrow (local) energy levels. With increasing the iron concentration, the states in near the Fermi region are blurred into the *d*-impurity band which is also a direct indication of the *d*–*f*-exchange interaction between the impurity and matrix electrons, which leads to an increase in the Curie temperature. From the foregoing, it is easy to see that the results of the latest quantum-chemical calculations of the electronic band structure of the $Eu_{1-x}Fe_xO$ solid solution, which is one of the structural components of the EuO : Fe composite, are in surprisingly good agreement with its experimentally established magnetic, optical and resonance characteristics. Although the entire complex of features of the electronic parameters of the composite given in Sections 2 and 3, only to the indicated solid solution, without taking into account the contributions of all its other structural components, is an illegal occupation. Let us trace this, in particular, on two characteristic examples.

The first one relates to the data of the NGR-studies of the EuO : Fe composite (Fig. 10) and the possibility of carrying out an "induction" effect in it – electron density transfer from Eu^{2+} ions to impurity ions embedded in the matrix lattice. The presence of such a transfer, which can be interpreted as the transition of a part of the europium ions Eu^{2+} to the Eu^{3+} state, and some iron ions to the Fe^+ state, does not contradict the results of calculations of the electronic band structure of the solid solution, although they do not directly follow from them. To clarify this not-so-obvious fact in [28] on an enlarged scale, the density of electronic states near the Fermi level of SS is given for a composition with 12.5 at.% iron.

It can be seen from this data that the position of the Fermi level does not coincide with the edge of the 4*f*-state band. Approximately 0.03 of the 4*f*-states (per europium atom) remain empty. On the other hand, it can be noted that the band of 3*d*-states of iron (with a negative value of the spin projection, spin-down) is asymmetric relative to the Fermi level, i.e., the number of states occupied by electrons (to the left of the Fermi energy) is somewhat larger (their zeroing corresponds to an energy of -0.15 eV) than the number of empty states in this zone (to the right of the Fermi energy, zeroing at 0.1 eV). Both of these circumstances indicate that there is actually a slight transfer of the electron density from the $4fEu^{2+}$ state to the $3dFe^{2+}$ state (about 0.03 electron per impurity Fe-node).

The latest calculations, like the vast majority of similar calculations by the methods of the electron density functional theory, refer to the temperature of $T = 0$ K. Obviously, a certain "smearing" of the Fermi level with increasing temperature roughly should be accompanied by a somewhat higher transfer of the electron density from 4*f*Eu-states to 3*d*Fe states. We note, however, that

the number of electrons transferred as a result of this effect to iron ions will be proportional to its concentration in the matrix. It follows that for small (by the order of a few percent) degrees of substitution of europium atoms by iron atoms, one cannot expect that the concentration of Eu^{3+} ions will be comparable with the concentration of Eu^{2+} ions in the composite, as takes place in case of the experiment (Fig. 11). This contradiction can be explained if it is assumed that higher Eu_2O_3 oxide nanoparticles are present in the structure of the EuO : Fe composites studied earlier, which are not detected by *X*-ray diffraction because of their small size, but can be identified by *X*-ray spectral methods. Arguments in favor of the existence of such aggregates have been repeatedly cited in the literature, for example, in studies of the properties of photocatalytic oxides doped with *3d*-elements. Thus, in [38], based on the study of *X*-ray absorption spectra, it was shown that when doping rutile with vanadium together with the formation of a solid solution V_2O_5 aggregates are also formed. Similarly, nanoparticles of oxides are formed also upon alloying rutile with iron, chromium, cobalt. In [39], using the *X*-ray emission spectroscopy method, it was shown that at the anatase is doped by chromium, the Cr_2O_3 nanoparticles are appearing in its structure, and in [40] it was established that the experimental spectra of optical absorption of iron-doped anatase can be explained by the presence of hematite or ilmenite nanoparticles. As for Fe-doped europium monoxide we know of only one work [41] in which it was shown by *X*-ray absorption spectroscopy that up to 10% of europium ions in the monoxide of the $EuO_{1.04}$ composition are in the oxidation state of 3^+ which agrees with the ideas that the monoxide of this composition contains an admixture of the Eu_2O_3 phase.

The second example concerns the experimental data of Fig. 7 – the presence of a "blocking" temperature – the spin reorientation of the magnetic moments of free iron nanoparticles in the composite structure and the transition to a superparamagnetic state at $T > 25$ K. Such a spin reorientation is in many ways analogous to spin-orientation transitions in rare-earth metals observed at low temperatures [42]. Nevertheless, the very indication of the theory of the antiparallelity of the spins of iron particles in the SS with respect to the spin state of the Eu^{2+} cations at $T = 0$ K implies the presence of T_{bl} at $T > 0$ K. What also can be attributed to the merit of the calculations.

Thus, the comparison of calculation results of the electronic band structure of the $Eu_{1-x}Fe_xO$ SS with the experimental data of the EuO : Fe spintronic composite, which is one of its structural constituents, is indicative of both surprisingly good agreement between each other and a correct and justified choice of theoretical model for doping a monoxide lattice, and the method used at calculating its electronic band structure.

It is shown that iron cations in the SS are at a high spin state, $1.7\mu_B$ higher than the intrinsic magnetic moment of pure iron. It is also shown that iron and europium cations in the monoxide structure have an oxidation degree close to 2^+. Both in pure and in Fe-doped monoxide, the states near the bottom of the conduction band (the 5*d*-state of europium) are 100% spin-polarized. It is shown that in Fe-doped monoxide there is an insignificant electron density transfer from Eu^{2+} ions to Fe^{2+} ions, but the main factor ensuring the presence of Eu^{3+} ions observed in the experiments is apparently the presence of Eu_2O_3 nanoclusters in the composite structure. Their presence, as well as the presence of superparamagnetic α-iron nanoparticles, apparently provide the samples of this composite in the bulk and thin-film states with long-term chemical stability and temporal stability of their physical parameters under normal conditions, as evidenced by the available experience with this spintronic material [43].

5. Conclusion. The EuO : Fe spintronic in contact with a nonmagnetic semiconductor

The above results of experimental and theoretical studies of the EuO : Fe ferromagnetic semiconductor composite served as the basis for modeling the operation of a spintronic contact device with its participation – as an electron injector (emitter) in a non-magnetic semiconductor *n*-GaAs (collector) capable of spin current transfer at room temperature. Such a structure can be used as the basis for the creation of a high-temperature field spin transistor [44]. Its creation on the basis of a contact of (EuO : Fe)/GaAs involved a process based on the use of industrial microelectronics technologies in designing similar devices and integrated circuits: on single-crystal *n*-GaAs plate with a carrier density of $n \approx 10^{14}$ cm^{-3} a composite layer of (EuO : Fe) up to 0.2 μm thick was deposited, which served as an emitter (injector) of spins. Contacts to the emitter and collector were made of gold. The magnetization and volt-ampere characteristic of individual contact structures at room temperature were measured. The behavior of the first characteristic corresponds to the data in Fig. 6. At saturation, the eigenvalue of the magnetic moment of the structure was in the range of $M \approx 40$ emu/g.

The current-voltage characteristic of the contact structure in absence of external magnetic field and in the state of its magnetization in a field of $H = 200$ mT is shown in Fig. 14. In the absence of an external magnetic field with an unmagnetized emitter, this characteristic is similar to the one observed in the operation of a conventional field MOS-transistor. In case of magnetization of the emitter, the current in the collector appears even at zero bias and in its magnitude it is inferior to the collector current at $H = 0$. In other words, it is determined by the spin component of the tunnel current, which coincides with the direction of the magnetization of the emitter – the spin injector. With the bias voltage applied to the contact, the magnitude of the spin current decreases.

If we consider the current through the collector in the unmagnetized state of the emitter as 100% charge current

transfer (J_0), then the degree of spin transfer (P) from the magnetized emitter (J_H) can be estimated from the relation:

$$P = (J_0 - J_H)/(J_0 + J_H). \quad (3)$$

According to Fig. 14, it reaches a value of $P \approx 60\%$, i.e. is very significant and, apparently, is largely determined by the $Eu_{1-x}Fe_xO$ (or the SS) – component of the composite – the emitter of the spins. This result, along with the magnetic and NGR investigations of the composite, as well as the analysis of the results of theoretical calculations of its electronic band structure, can serve as one more indirect proof of the above-mentioned physical mechanisms that contribute to the increased values of the magnetic moment of the emitter at room temperatures. It can be assumed that in this case the temperature factor (lattice vibrations of the structural components of the contact) does not have a significant effect on the possible spin-flip of the charge carriers. The interface layer of the collector is also transparent for them. The mechanism of such a high-magnitude spintrance in case under consideration is ensured by the wide-band structure of the injector and collector of forbidden zones composing the planar structure. When the relationship between their values is fulfilled: E_g (GaAs) $\geq E_g$ (EuO).

The supply of voltage to the contact structure may well cause electronic transport from the injector and with a different spin orientation of the carriers. In addition, in this device, crystal-structural nonidentity of the injector and detector materials is also possible (the symmetry of the crystal cells and their parameters is different), which is also capable of being an additional cause of the spin flip at the boundary of the interface and a decrease of a degree of the spin current transfer, P. Even with such a minimum difference in the lattice parameters of the EuO (1) and GaAs (2) crystals, $a1/a2 = 0.176$ (or 17%). Nevertheless, remaining unusually high and record-breaking in terms of the degree of spintrance among the spintronic contacts created, it allows us to believe that using parameters of europium monoxide, which are record for ferromagnets, partially retained at high (room) temperatures in the EuO : Fe composite, the further prospect of implementing spin current transfer in such transistor becomes obvious [44, 45]. This is promoted by the search for semiconducting crystals featuring a high g-factor of current carriers as the latter determines the value of Zeeman splitting of extrinsic electronic levels in the forbidden gap since $\Delta = \mu_B gH$. For instance, $\Delta = 50$ K for n-InSb crystal with $g = 52$ in the field of $H = 1$ T and $\Delta = 1$ K for silicon with $g = 2$. That is, according to these parameters such material is unlikely to be used as a carrier of spin information and quantum memory cells. Naturally, the existing experience and practice of developing information systems based on Si-technologies will be used in the creation of new spintronics technologies, which are the microelectronics of the XXI century.

References

1. Žutić I., Fabian J., Das Sarma S. Spintronics: fundamentals and applications. *Rev. Mod. Phys.*, 2004; 76(2): 323. https://doi.org/10.1103/RevModPhys.76.323
2. Lashkarev G.V., Radchenko M.V., Karpina V.A., Sichkovsky, V.I. Deluted magnetic semiconductors as materials for spintronics. *Fizika Nizkikh Temperatur*, 2007; 33(2/3): 228–238. https://doi.org/10.1063/1.2409655
3. Ivanov V.A., Aminov T.G., Novotortsev V.M., Kalinnikov V.T. Spintronics and spintronics materials. *Russ. Chem. Bull.*, 2004; 53(11): 2357–2405. https://doi.org/10.1007/s11172-005-0135-5
4. Matsumoto Y., Murakami M., Shono T., Hasegawa T., Fukumura T., Kawasaki M., Ahmet P., Chikyow T., Koshinara S.., Koinuma H. Room-temperature ferromagnetism in transparent transition metal-doped titanium dioxide. *Science*, 2001; 291(5505): 854–856. https://doi.org/10.1126/science.1056186
5. Chambers S.A., Thevuthasan S., Farrow R.F.C., Marks R.F., Thiele J.U., Folks L., Samant M.G., Kellock A.J., Ruzycki N., Ederer D.L., Diebold U. Epitaxial growth and properties of ferromagnetic co-doped TiO_2 anatase. *Appl. Phys. Lett.*, 2001; 79(21): 3467–3469. https://doi.org/10.1063/1.1420434
6. Park W.K., Ortega-Hertogs R.J., Moodera J.S., Punnoose A., Seehra M.S. Semiconducting and ferromagnetic behavior of sputtered co-doped TiO_2 thin films above room temperature. *J. Appl. Phys.*, 2002; 91(10): 8093–8095. https://doi.org/10.1063/1.1452650
7. Stampe P.A., Kennedy R.J., Xin Y., Parker J.S. Investigation of the cobalt distribution in the room temperature ferromagnet TiO_2:Co. *J. Appl. Phys.*, 2003; 93(10): 7864. https://doi.org/10.1063/1.1556119
8. Fukumura T., Yamada Y., Tamura K., Nakajiama K., Aoyama T., Tsukazaki A., Sumiya M., Fuke S., Segawa Y., Chikyow T. Magneto-optical spectroscopy of anatase TiO_2 doped with Co. *Jpn. J. Appl. Phys.*, 2003, 42(2A): 105. https://doi.org/10.1143/JJAP.42.L105
9. Chambers S.A., Droubay T., Wang C.M., Lea A.S., Farrow R.F.C., Folks L., Deline V., Anders S. Clusters and magnetism in epitaxial co-doped TiO_2 anatase. *Appl. Phys. Lett.*, 2003; 82(8): 1257. https://doi.org/10.1063/1.1556173
10. Kim J.-Y., Park J.-H., Park B.-G., Noh H.-J., Oh S.-J., Yang J.S., Kim D.-H., Bu S.D., Noh T.-W., Lin H.-J., Hsieh H.-H., Chen C.T. Ferromagnetism induced by clustered Co in co-doped anatase TiO_2 thin films. *Phys. Rev. Lett.*, 2003; 90(1): 017401. https://doi.org/10.1103/PhysRevLett.90.017401
11. Chambers S. A potential role in spintronics. *Mater. Today*, 2002; 5(4): 34–39. https://doi.org/10.1016/S1369-7021(02)05423-8
12. Balagurov L.A., Klimonsky S.O., Kobeleva S.P., Orlov A.F., Perov N.S., Yarkin D.G. On the origin of ferromagnetism in semiconducting $TiO_{2-\delta}$:Co oxide. *JETP Lett.*, 2004; 79(2): 98–99. https://doi.org/10.1134/1.1690360
13. Nipan G.D., Stognij A.I., Ketzko V.A. Oxide ferromagnetic semiconductors: coatings and films. *Russ. Chem. Rev.*, 2012; 81(5): 458–475. https://doi.org/10.1070/RC2012v081n05ABEH004251

14. Ignat'eva N.I. Proceedings of the 3rd International Conference "Micro- and Nanoelectronics – 2003", Kislovodsk, 2003: 5. (In Russ.)
15. Borukhovich A.S., Ignat'eva N.I., Bamburov V.G. Ferromagnetic composite material for spintronics. *Doklady Physics*, 2005; 50(5): 239–240. https://doi.org/10.1134/1.1941496
16. Ignateva N.I., Boruhovich A.S., Bamburov V.G. Composite magnetic EuO/Fe materials. *Perspektivnye Materialy*, 2005; (5): 68–71. (In Russ.)
17. Bamburov V.G., Borukhovich A.S., Samokhvalov A.A. *Vvedenie v fizicheskuyu khimiyu ferromagnitnykh poluprovodnikov* [Introduction in physical chemistry of ferromagnet semiconductors]. Moscow: Metallurgiya, 1988: 206. (In Russ.)
18. Borukhovich A.S., Galyas A.I., Demidenko O.F., Dyakonov V., Ketsko V.A., Ignat'eva N.I., Novitskii N.N., Stognij A.I., Szymczak H., Yanushkevich K.I. The production and structure of submicrometer $Eu_{0.75}Fe_{0.25}O$ films on InSb, Si, and GaAs substrates. *Inorg. Mater.*, 2009; 45(3): 254–257. https://doi.org/10.1134/S0020168509030066
19. Ahn K.A., Shafer M.W. Relationship between stoichiometry and properties of EuO films. *J. Appl. Phys.*, 1970; 41(3): 1260. https://doi.org/10.1063/1.1658902
20. Patent 2291134 (RF). *Spintronnyi kompozitsionnyi material* [Spintronic composite material]. A.S. Borukhovich, N.I. Ignat'eva, V.G. Bamburov, 2006. (In Russ.)
21. Altshuler T.S., Goryunov Yu.V., Bresler M.S. Ferromagnetic ordering of iron impurities in the mixed-valence semiconductor SmB_6. *Phys. Rev. B*, 2006; 73(23): 235210. https://doi.org/10.1103/PhysRevB.73.235210
22. Patent 2360317 (RF). *Sposob polucheniya tonkoplenochnogo oksidnogo materiala, legirovannogo ionami ferromagnitnogo metalla, dlya spintroniki* [Method of obtaining of the thin film oxide material for spintronics]. A.S. Borukhovich, N.I. Ignat'eva, A.I. Galyas, O.F. Demidenko, F.I. Stognij, K.I. Yanushkevich, 2009. (In Russ.)
23. International Centre for Diffraction Data. PCPDFWIN, JCPDS, 1998; 2(15): 0886. URL: https://www.icdd.com/
24. Borukhovich A.S., Ignat'eva N.I., Galyas A.I., Demidenko O.F., Fedotova Yu.A., Stognii A.I., Yanushkevich K.I. Superparamagnetism of the ferromagnetic composite material EuO:Fe for spintronics. *J. Nanoelectron. Optoelectron*, 2008; 3(1): 82–85. https://doi.org/10.1166/jno.2008.009
25. Borukhovich A.S., Ignat'eva N.I., Yanushkevich K.I., Stognii A.I., Fedotova Yu.A. Mössbauer spectroscopy study of the EuO : Fe spintronic material. *JETP Lett.*, 2009; 89(4): 191–193. https://doi.org/10.1134/S0021364009040067
26. Nemov S.A., Marchenko A.V., Seregin P.P., Tomil'tsev E.A. Europium(II) in glasses of the Al_2O_3-SiO_2-MnO-Eu_2O_3 system. *Glass Phys. Chem.*, 2007; 33(6): 658–660. https://doi.org/10.1134/S1087659607060181
27. Tanaka K., Tatehata N., Fujita K., Hirao K. Preparation and Faraday effect of EuS microcrystal-embedded oxide thin films. *J. Appl. Phys.*, 2001; 89(4): 2213–2219. https://doi.org/10.1063/1.1339217
28. Anoshina O.V., Zhukov V.P., Borukhovich A.S. Electronic band structure and properties of the solid solution $Eu_{1-x}Fe_xO$. *Phys. Solid State*, 2015; 57(11): 2173–2178. https://doi.org/10.1134/S1063783415110037
29. Perdew J.P., Burke K., Ernzerhof M. Generalized gradient approximation made simple. *Phys. Rev. Lett.*, 1996; 77(18): 3865–3868. https://doi.org/10.1103/PhysRevLett.77.3865
30. An J.M., Barabach S.V., Osolins V., van Schilfgaarde M., Belashchenko K.D. First-principles study of phase stability of Gd-doped EuO and EuS. *Phys. Rev. B*, 2011; 83(6): 064105. DOI: 10.1103/PhysRevB.83.064105
31. An J.M., Belashchenko K.D. Electronic structure and magnetic properties of Gd-doped and Eu-rich EuO. *Phys. Rev. B*, 2013; 88(5): 054421. https://doi.org/10.1103/PhysRevB.88.054421
32. Anisimov V.I., Solovyev I.V., Korotin M.A., Czyżyk M.T., Sawatzky G.A. Density-functional theory and NiO photoemission spectra. *Phys. Rev. B*, 1993; 48(23): 16929. DOI: 10.1103/PhysRevB.48.16929. https://doi.org/10.1103/PhysRevB.48.16929
33. Novotny Z., Mulakaluri N., Edes Z., Schmid M., Pentcheva R., Diebold U., Parkinson G.S. Probing the surface phase diagram of Fe_3O_4(001) towards the Fe-rich limit: Evidence for progressive reduction of the surface. *Phys. Rev. B*, 2013; 87(19): 195410. https://doi.org/10.1103/PhysRevB.87.195410
34. Steeneken P.G., Tjeng L.H., Elfimov I., Sawatzky G.A., Ghiringhelli G., Brookes N.B., Huang D.-J. Exchange splitting and charge carrier spin polarization in EuO. *Phys. Rev. Lett.*, 2002; 88(4): 047201. https://doi.org/10.1103/PhysRevLett.88.047201
35. Borukhovich A. S. *Fizika materialov i struktur sverkhprovodyashchei i poluprovodnikovoi spinovoi elektroniki* [Physics of Materials and Structures of Superconducting and Semiconducting Spin Electronics]. Ekaterinburg: UB RAS, 2004, p. 175. (In Russ.)
36. Eastman D.E., Holtzberg F., Methfessel S. Photoemission studies of the electronic structure of EuO, EuS, EuSe, and GdS. *Phys. Rev. Lett.*, 1969; 23(5): 226. https://doi.org/10.1103/PhysRevLett.23.226
37. Auslender M. I., Irkhin V. Yu. The spin polarization of conduction electrons in ferromagnetic semiconductors. *Solid State Comm*., 1984; 50(11): 1003–1005. https://doi.org/10.1016/0038-1098(84)90275-8
38. Gracia F., Holgado J.P., Caballero A., Gonzalez-Elipe A.R. Structural, optical, and photoelectrochemical properties of M^{n+}–TiO^2 model thin film photocatalysts. *J. Phys. Chem. B*, 2004; 108(45): 17466–17476. https://doi.org/10.1021/jp0484938
39. Zhu J.F., Deng Z.G., Chen F., Zhang J.L., Chen H.J., Anpo M., Huang J.Z., Zhang L.Z. Hydrothermal doping method for preparation of Cr^{3+}-TiO_2 photocatalysts with concentration gradient distribution of Cr^{3+}. *Applied Catalysis B: Environmental*, 2006; 62(3-4): 329–335. https://doi.org/10.1016/j.apcatb.2005.08.013
40. Krasil'nikov V.N., Zhukov V.P., Perelyaeva L.A., Baklanova I.V., Shein I.R. Electronic band structure, optical absorption, and photocatalytic activity of iron-doped anatase. *Phys. Solid State*, 2013; 55(9): 1903–1912. https://doi.org/10.1134/S1063783413090199
41. Ignat'eva N.I., Shkvarin A.S., Osotov V.I., Finkel'shtein L.D. Europium valence state in europium monoxide-iron (cobalt) magnetic composites. *Russ. J. Inorg. Chem.*, 2009; 54(10): 1517–1521. https://doi.org/10.1134/S0036023609100027
42. Belov K.P., Zvezdin A.K., Kadomtseva A.M., Levitin R.Z. *Orientatsionnye perekhody v redkozemel'nykh magnetikakh* [Orientational Transitions in Rare Earth Magnetics]. Moscow: Nauka, 1979: 317. (In Russ.)
43. Borukhovich A.S., Ignat'eva N.I. *J. Spintronics & Quantum Electronics*, 2018; 1(1): 11.
44. Borukhovich A. Spin transfer in EuO:Fe/GaAs contact. *J. Modern Phys*., 2013; 4(3): 306–310. https://doi.org/10.4236/jmp.2013.43041
45. Borukhovich A.S., Troshin A.V. Europium Monoxide: Semiconductor and Ferromagnet for Spintronics. Cham: Springer, 2018; 265: 189. https://doi.org/10.1007/978-3-319-76741-3